Marine Structures 58 (2018) 53–72

Contents lists available at ScienceDirect

Marine Structures

journal homepage: www.elsevier.com/locate/marstruc

Global slamming forces on jacket structures for offshore wind applications

Ying Tu[a], Zhengshun Cheng[b,*], Michael Muskulus[a]

[a] Department of Civil and Environmental Engineering, Norwegian University of Science and Technology, Høgskoleringen 7A, 7491 Trondheim, Norway
[b] Department of Marine Technology, Centre for Autonomous Marine Operations and Systems, Norwegian University of Science and Technology, Otto Nielsens veg 10, 7491 Trondheim, Norway

ARTICLE INFO

Keywords:
Wave slamming force
Jacket structure
Experimental study
Statistical analysis
Slamming coefficient
Force model
Plunging breaking wave

ABSTRACT

This study investigates the global slamming forces due to plunging breaking waves on a jacket structure, based on the statistical analysis of the experimental data from the WaveSlam project. Hammer tests and wave tests were conducted in the project, and the data are used to reconstruct the time series of the global slamming force by employing a method based on linear regression. The used wave test data were acquired under one wave condition. A total of 3910 force time series are reconstructed and analyzed statistically to reveal the characteristics of the slamming force. For each force time series, six parameters are introduced to describe it, including the peak force, duration, impulse and rising time, etc. The variability and correlation of these parameters are investigated. The distribution of these parameters is modeled with various probability distributions. The results show the high variability of the slamming force and the importance of statistical analyses. Based on these statistical analyses, the slamming coefficient is estimated from the peak force. For a curling factor of 0.4, the mean slamming coefficient is about 1.29. When considering one standard deviation around the mean, the slamming coefficient varies from 0.70 to 6.78 for a curling factor ranging from 0.1 to 0.5. A representative time series of wave slamming force is obtained by averaging the individual force time series. Accordingly, a 3-parameter triangular force model and a 5-parameter exponential force model are proposed to describe the development of the slamming force in time.

1. Introduction

Currently, the substructures supporting offshore wind turbines are usually bottom-fixed structures, such as monopiles, tripods, jackets, gravity based structures, etc. In certain sea environments, they are exposed to plunging breaking waves at some locations, which leads to slamming forces. Such kind of slamming forces have been identified based on the recorded sea state conditions and associated structural responses for a 2 MW wind turbine mounted on a monopile at the Blyth wind farm off the coast of England [1]. Slamming forces can affect the performance and fatigue life of the substructures for offshore wind turbines. They should therefore be considered in the design of offshore wind turbines, as recommended by various standards and guidelines [2–4].

Slamming is a strongly nonlinear phenomenon that usually causes an extremely high impact force within a very short time [5,6]. In the past decades, a large amount of efforts have been devoted to investigate slamming forces theoretically, numerically and experimentally. Theoretical analysis is usually based on the von Karman or the Wagner impact model together with several reasonable assumptions [5,7], and numerical studies on slamming forces use Computational Fluid Dynamics (CFD), considering either

* Corresponding author.
E-mail address: zhengshun.cheng@ntnu.no (Z. Cheng).

https://doi.org/10.1016/j.marstruc.2017.11.001
Received 19 December 2016; Received in revised form 31 May 2017; Accepted 7 November 2017

inviscid or viscid flows [6,8]. Due to the strong nonlinearities of slamming forces, small-scale experiments or full-scale field measurements seem to be the most reliable method to quantify them. To date, several experimental studies of slamming forces on vertical or inclined slender cylindrical structures have been carried out [9–11]. An on-site measurement regarding the slamming loads has also been conducted for a monopile wind turbine at the Blyth wind farm [1].

Most of the aforementioned studies on slamming forces are with respect to slender cylindrical structures, and the results can be used for the design of monopiles. Truss structures, such as jackets, are also a promising support structure concept for offshore wind turbines, especially in intermediate water. Because of the presence of several legs and braces, the waves approaching the hind legs and braces are affected by the front ones. This will result in a more complicated slamming scenario than that of the monopiles. Nevertheless, investigations of the slamming forces on jacket structures are still limited in number to date. The WaveSlam project[1] was initiated to bridge this knowledge gap. Using a 1:8 model of a jacket structure typical for offshore wind applications, the project is the first one at this scale and for this kind of structures.

Several other studies have been conducted to investigate the slamming forces on jacket structures based on the experimental data from the WaveSlam project. Rausa et al. [12] studied breaking wave forces on the front bracings of the jacket structure with a finite element model by assuming a triangular time history of wave slamming forces. A fitting procedure was then applied to match the result from the finite element model with the experimental data. Tu et al. [13] investigated the slamming loads on the bracings of the jacket structure based on local force data. An optimization-based deconvolution (ODC) method, which used the linearity of the structure, was proposed for the estimation. However, the methods used in these studies are only able to calculate the peak forces based on additional assumptions (e.g. assuming a triangular shape force model, which is not validated) or the impulses of the loads. The time series of the forces, which are necessary for the force analysis, were not resolved.

To obtain the time series of wave slamming forces, Jose et al. [14] applied Empirical Mode Decomposition (EMD) to analyze the total slamming force and the Frequency Response Function method to analyze the local slamming force on the jacket structure. Tu et al. [15] employed the regularization method, which is a classical inverse method, to develop two approaches for the reconstruction of the local slamming force time series. The method by Tu et al. [15] takes the structure property into consideration and can provide an easily applicable solution for the inverse estimation of slamming loads.

In this study, the slamming force estimation method proposed by Tu et al. [15] was further applied to reconstruct the global slamming force time series using the data set from the WaveSlam project. Six parameters were introduced to describe the global slamming force time series, such as the peak force, duration, total impulse, etc. The variation, correlation and distribution features of these parameters were investigated to reveal the characteristics of the global slamming force under one wave condition. A representative slamming force time history and the slamming coefficient were then estimated. Based on the representative time history, two slamming force models are proposed, which provide potential means to properly account for slamming forces in the future design of jacket structures.

2. Experiment and data

WaveSlam is a research project that aims to improve the method for calculating forces from plunging breaking waves on jacket structures through model tests on a large scale [16]. The project was conducted by a consortium headed by the University of Stavanger (UiS) and the Norwegian University of Science and Technology (NTNU) in 2012–2013. The jacket model used in the experiment was similar to the structure designed by Reinertsen AS for the Thornton Bank offshore wind farm [17]. Following the earlier small scale (1:50) model tests at NTNU [18], a 1:8 scale model of the jacket structure was constructed, and the experiment was carried out in summer 2013 using the Large Wave Flume facilities at the Coastal Research Centre (Forschungszentrum Küste, FZK)[2], Hannover, Germany. The data is now publicly available.

2.1. Experimental setup

The setup of the experiment is demonstrated in Fig. 1. The wave flume is approximately 300 m long, 5 m wide and 7 m deep. The waves were generated by the wave board at the left end of the flume, went over a 1:10 slope, then reached the jacket model on a 2.3 m high plateau. A water depth of 16 m was simulated, but the water depth at the jacket model was adjusted slightly to be 1.8 m (instead of 2.0 m) for some test cases. The legs and braces of the jacket model were both 0.14 m in diameter.

A global coordinate system is defined as following: The origin is at the center of the wave board and at the bottom of the wave flume. The x-axis is positive in the wave direction. The z-axis is positive upwards. The y-axis forms a right hand system with the other axes.

Wave gauges were installed at 15 different locations. Three Acoustic Doppler Velocity meters (ADVs) were installed in the plane of the legs. The motion of the wave paddle was also recorded. The jacket was equipped with four total force transducers, ten local force transducers on the legs, twelve XY force transducers on the braces, and four one-directional accelerometers.

The measurements taken by the total force transducers are essential in this study to investigate the global slamming forces. As shown in Fig. 2, there were two total force transducers installed at the top of the jacket model and two installed at the bottom of the jacket model. The structure was hung from the top and did not touch the ground during the tests. The measured forces are in global x

[1] http://hydralab.eu/research–results/ta-projects/project/19/; December 2016.
[2] https://www.fzk.uni-hannover.de/; December 2016.

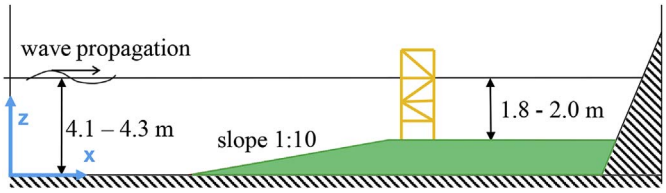

Fig. 1. Experimental setup and global coordinates.

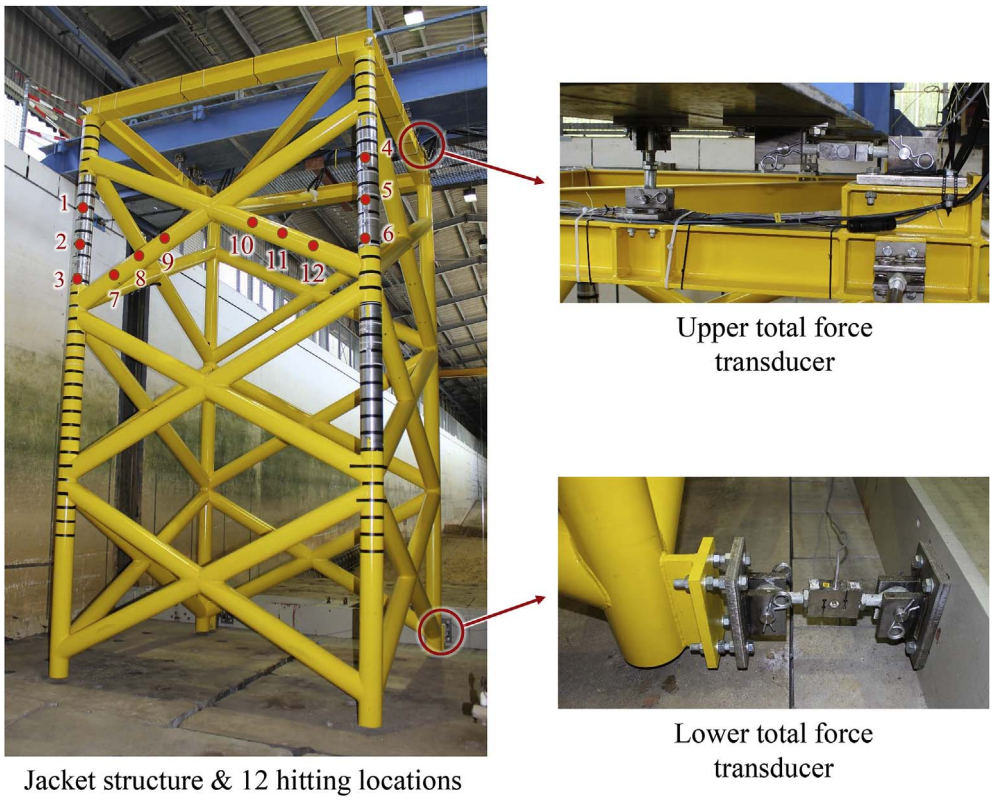

Fig. 2. Jacket structure, hammer hitting locations and total force transducers. Figures reprinted with permission from the WaveSlam project.

direction (wave direction) and have a sampling frequency of 10 kHz. The details of the transducers are illustrated in the figure as well. The names and locations of the transducers are introduced in Table 1. The local force measurements are not used in this study, so the locations of those transducers are not shown in the figure.

2.2. Wave test cases

Five wave cases repeated with exactly the same preset condition were selected for the investigation. The cases and the test condition are shown in Table 2. The waves are regular shallow water plunging breaking waves. The break points of the waves are approximately in the plane of the front legs of the jacket. The wave heights at the structure were taken from the measurement, so the values are slightly different from case to case.

Table 1
Total force transducers and their locations in global coordinates.

Transducer	Description	x [m]	y [m]	z [m]
FTTF01	Total force bottom south	200.961	1.405	2.465
FTTF02	Total force top south	200.265	1.405	6.935
FTTF03	Total force bottom north	200.961	3.655	2.465
FTTF04	Total force top north	200.265	3.655	6.935

Table 2
Wave test cases.

Condition	Value
ID of test run	20130617.15 ~ 19
Number of runs	5
Number of waves per run	20
Wave height	1.5 m
Wave height at structure	1.809 ~ 1.833 m
Wave period	4.9 s
Depth	4.3 m
Depth at structure	2.0 m
Run type	Regular
Breaking location	At front legs

2.3. Hammer test cases

Apart from the wave test data, hammer test data are also essential to reconstruct the slamming forces. During the hammer tests, the structure was hit by a 1.5 kg impulse hammer in the wave direction. The impulse hammer recorded the time series of the forces exerted on the structure with a sampling frequency of 9600Hz, in addition to the measurements mentioned in Section 2.1. The selected hammer test cases shown in Table 3 were all carried out in water. The water depth was 2 m to match the wave cases. The hammer hit at twelve locations in the front side of the structure, both on the braces and on the legs. These locations (see Fig. 2) are in or close to the expected wave slamming zone for the wave tests. Since the hammer impacts were exerted manually, the locations shown in the figure are approximate. Data for different number of hits are available for different locations as shown in Table 3.

3. Calculation of wave slamming forces

3.1. Pre-processing of the data

Given the raw measurement data, some pre-processing is necessary before they can be used to calculate the slamming forces. A bandpass filter was used to eliminate the high frequency noise in the measurements and to only preserve the signal from 0 to 300Hz. The effect of the filtering is shown in Fig. 3. Since the transducers were not always precisely calibrated to zero before each test, the measured forces were subtracted by the mean values of the measurement over some seconds at calm status in the same run. The forces measured by the four transducers were summed up to obtain the total forces as shown in Fig. 4. The first natural frequency of the jacket structure in water is determined by spectral analysis of the hammer response data, the value of which is 25.2 Hz. The impulse hammer measurements were resampled to 10 kHz to match the total force measurements.

The force exerted by a breaking wave on a structure is composed of two parts: a quasi-static force $f_{qs}(t)$ and an impact force by the breaker, namely the slamming force $f_s(t)$. Therefore, a measured response force due to this wave also has two parts: a quasi-static part caused by $f_{qs}(t)$ and a dynamic part caused by $f_s(t)$. The dynamic part should be extracted, so that it can be used to reconstruct the slamming force.

Two common methods to achieve this goal are frequency domain filtering and Empirical Mode Decomposition (EMD) combined with filtering [10]. However, these methods overestimate the quasi-static part in the region of the maximum load [10], thus leading to underestimation of the dynamic part.

A time domain robust LOESS smoother [19] is used in this study to estimate the quasi-static part. The dynamic part equals the total response force minus the quasi-static part. The smoothing method is realized by local regression using weighted linear least squares and a 2nd degree polynomial model. The method assigns zero weight to the data outside six mean absolute deviations. The

Table 3
Hammer test cases.

Hit location number	Total hammer hits	ID of test run
1	6	24062013.14 ~ 16
2	4	24062013.17 ~ 18
3	4	24062013.22 ~ 23
4	6	24062013.31 ~ 33
5	8	24062013.34 ~ 37
6	6	24062013.38 ~ 40
7	2	24062013.24
8	2	24062013.25
9	2	24062013.26
10	2	24062013.27
11	2	24062013.28
12	2	24062013.30

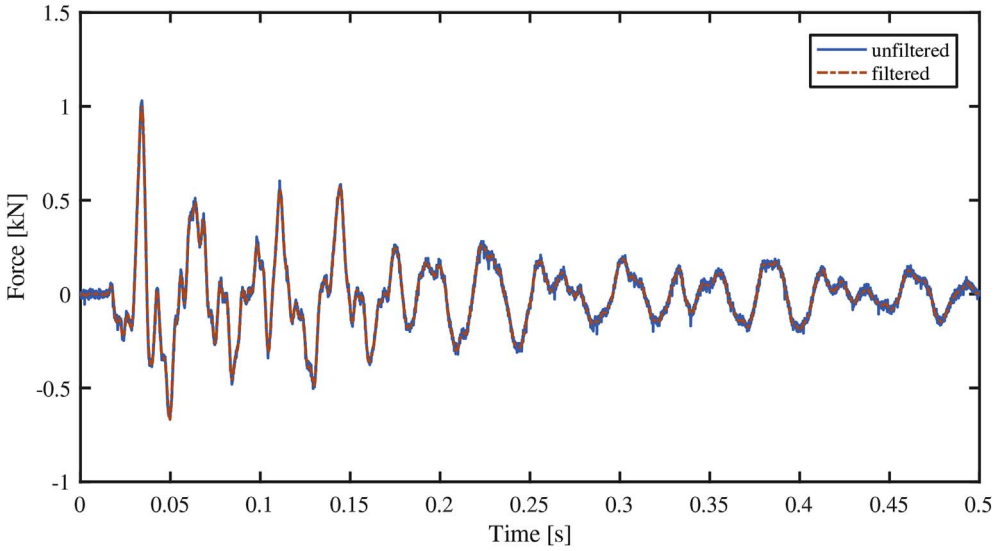

Fig. 3. Comparison of unfiltered and filtered forces measured by one transducer.

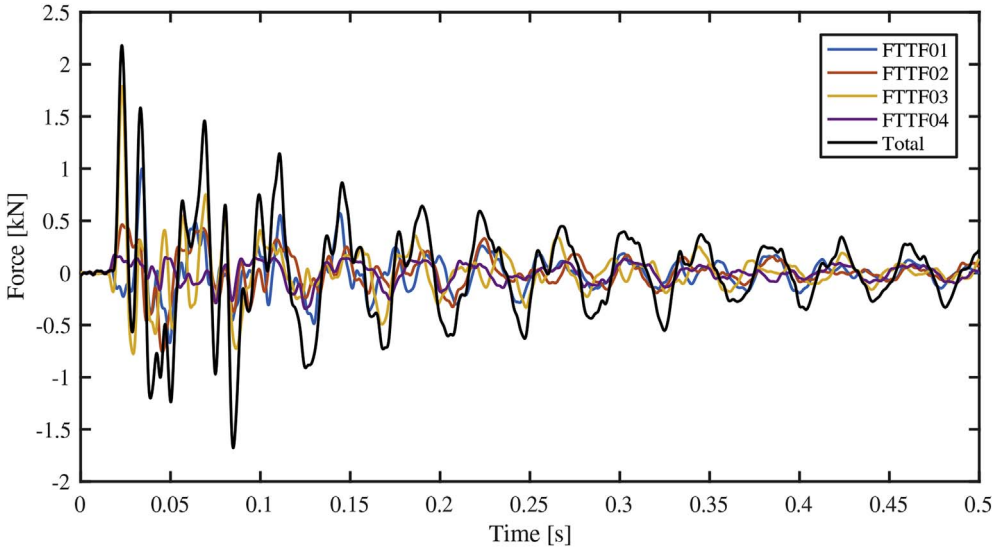

Fig. 4. Summation of the forces measured by four transducers.

smoothing span is set to be 5% of the total number of data points.

Fig. 5 shows one example where the method is applied. The response force has two peaks, because the wave hit the structure first on the front side and then again on the back side in the experiment. Only the first peak is used in this study, since the waves broke at the front legs. The general trend of the quasi-static part is captured very well by the method. There is no significant overestimation of the quasi-static part around the first peak, because the data points in this region are considered as outliers, and zero weight is assigned to them. For the second peak, the response force is caused by a mixture of two impacts and the separation may be inaccurate, but since we only focus on the first peak, it is not very important to have a precise separation after that.

3.2. Reconstruction of wave slamming forces

The idea of reconstructing wave slamming forces is to use the available response forces of the structure measured in the wave tests, and both the impact forces and response forces measured in the hammer tests to calculate the wave impact forces. This is an inverse problem and in general ill-defined. Therefore, additional assumptions must be made.

Ideally, a reference impact test that covers the whole wave slamming area would be most helpful for the reconstruction. In practice, the hammer tests could only be done for twelve discrete locations. Therefore, each response force from the wave test is combined with hammer test data from different hits at different locations for the reconstruction. The reconstructed forces are

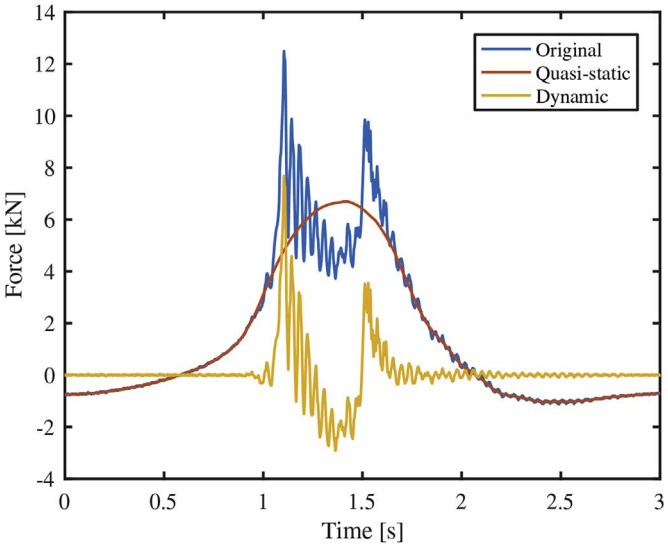

Fig. 5. Separation of quasi-static and dynamic parts in a total response force.

"effective forces", which means that the wave slam is assumed to occur only on the corresponding hammer impact location. The result obtained by using all such "wave-hammer data pairs" is analyzed further in later sections.

The hammer test data used for force reconstruction were acquired from the experiment with the structure in water. However, the change of water depth due to the existence of waves is not taken into account, due to the limitation of the data. The reconstruction inherently includes hydroelastic effects, since it employs experimental data that includes such effects. Loads on an ideal, rigid jacket structure are expected to be somewhat different. The structure model in the experiment has a high first eigenfrequency, which is not far from the frequency of typical slamming excitations. The hydroelastic effect caused thereby is expected to be stronger than that for a normal full-scale wind turbine jacket under slamming loads.

The wave test and hammer test data used for reconstruction have all been pre-processed according to Section 3.1. The reconstructed slamming forces are only in the wave direction due to the data properties.

For each wave-hammer data pair, the force reconstruction method proposed in Tu et al. [15] is used. It makes use of the linearity of the structure as discussed in Tu et al. [13].

The basic principle of the method is demonstrated in Fig. 6.

A wave slam on the structure is imagined as a hammer hitting one location on the structure with different amplitudes for multiple times.

Step 1 Knowing the response forces from one wave slam and from one hammer impact, the wave response force is decomposed into multiple hammer response forces scaled by corresponding coefficients.

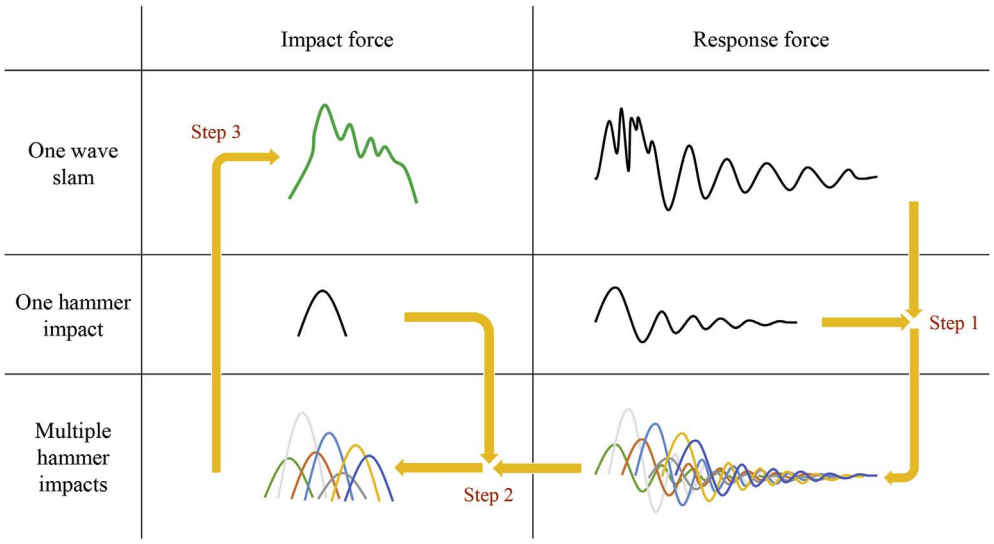

Fig. 6. Illustration of the force reconstruction method.

Step 2 Each hammer response force corresponds to one hammer impact force. So, the hammer impact forces, corresponding to the hammer response forces obtained from Step 1, are determined by using the same coefficients.

Step 3 Summing up the multiple hammer impact forces, the impact force from one wave slam is acquired.

For more detailed explanation, the wave slamming force is written as a vector

$$\mathbf{f_W} = \begin{pmatrix} f_{W_1} & f_{W_2} & f_{W_3} & \cdots & f_{W_n} \end{pmatrix}^T \tag{1}$$

It can be expressed as

$$\mathbf{f_W} = \mathbf{F_H}\,\boldsymbol{\beta} \tag{2}$$

where

$$\mathbf{F_H} = \begin{pmatrix} f_{H_1} & 0 & \cdots & 0 \\ \vdots & \vdots & \ddots & \vdots \\ f_{H_\delta} & 0 & \ddots & 0 \\ f_{H_{\delta+1}} & f_{H_1} & \ddots & 0 \\ \vdots & \vdots & \ddots & \vdots \\ f_{H_{(p-1)\delta}} & f_{H_{(p-2)\delta}} & \ddots & 0 \\ f_{H_{(p-1)\delta+1}} & f_{H_{(p-2)\delta+1}} & \ddots & f_{H_1} \\ \vdots & \vdots & \ddots & \vdots \\ f_{H_n} & f_{H_{n-\delta}} & \cdots & f_{H_{n-(p-1)\delta}} \end{pmatrix} \tag{3}$$

is composed of column vectors representing repeated and shifted hammer impact forces. The symbol p denotes the total number of hypothetical hammer hits. The symbol δ denotes the interval between every two hammer hits, and is named *step factor*. The step factor is set to be 5 for most cases, according to Tu et al. [15].

The coefficients

$$\boldsymbol{\beta} = \begin{pmatrix} \beta_1 & \beta_2 & \beta_3 & \cdots & \beta_p \end{pmatrix}^T \tag{4}$$

are given as a parameter vector for scaling the hammer hits.

The wave response force is written as

$$\mathbf{r_W} = \begin{pmatrix} r_{W_1} & r_{W_2} & r_{W_3} & \cdots & r_{W_n} \end{pmatrix}^T \tag{5}$$

It can be expressed as

$$\mathbf{r_W} = \mathbf{R_H}\,\boldsymbol{\beta} + \mathbf{e} \tag{6}$$

where

$$\mathbf{R_H} = \begin{pmatrix} r_{H_1} & 0 & \cdots & 0 \\ \vdots & \vdots & \ddots & \vdots \\ r_{H_\delta} & 0 & \ddots & 0 \\ r_{H_{\delta+1}} & r_{H_1} & \ddots & 0 \\ \vdots & \vdots & \ddots & \vdots \\ r_{H_{(p-1)\delta}} & r_{H_{(p-2)\delta}} & \ddots & 0 \\ r_{H_{(p-1)\delta+1}} & r_{H_{(p-2)\delta+1}} & \ddots & r_{H_1} \\ \vdots & \vdots & \ddots & \vdots \\ r_{H_n} & r_{H_{n-\delta}} & \cdots & r_{H_{n-(p-1)\delta}} \end{pmatrix} \tag{7}$$

is composed of column vectors representing repeated and shifted hammer response forces, and

$$\mathbf{e} = \begin{pmatrix} e_1 & e_2 & e_3 & \cdots & e_n \end{pmatrix}^T \tag{8}$$

is an error term due to the noise in the measurements.

An ordinary least squares regression technique is used to solve for the parameter vector $\boldsymbol{\beta}$ based on Eq. (6), so the estimated parameter vector is

$$\hat{\boldsymbol{\beta}} = \left(\mathbf{R_H^T R_H}\right)^{-1} \mathbf{R_H^T}\,\mathbf{r_W} \tag{9}$$

Applying $\hat{\boldsymbol{\beta}}$ to Eq. (2), the wave slamming force is estimated as

$$\hat{\mathbf{f_W}} = \mathbf{F_H}\,\hat{\boldsymbol{\beta}} \tag{10}$$

Applying $\hat{\boldsymbol{\beta}}$ to Eq. (6), the wave response force can be recalculated as

$$\hat{\mathbf{r_W}} = \mathbf{R_H}\,\hat{\boldsymbol{\beta}} \tag{11}$$

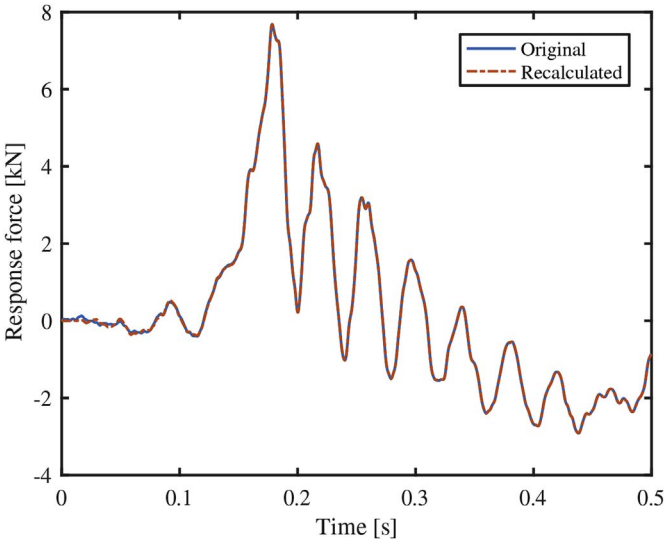

Fig. 7. Comparison of original and recalculated response forces.

A exemplary comparison between an original wave response force and the corresponding recalculated wave response force is shown in Fig. 7. Since the response forces match well, the estimated $\hat{\boldsymbol{\beta}}$ is deemed to be an appropriate representation of the slamming event. Using this $\hat{\boldsymbol{\beta}}$, the corresponding wave slamming force is estimated and shown in Fig. 8.

4. Statistical analysis of wave slamming forces

Using different combinations of the wave test data and the hammer test data described in Section 2, the wave slamming forces were reconstructed following the methods described in Section 3.

As stated in Section 2.2, the used wave test data were acquired from 5 runs with 20 waves in each run under the same preset conditions. Even under the same conditions, the waves in the tests were not exactly the same. Fig. 9 and Fig. 10 illustrate how the wave height and the wave period vary in the tests. The difference in the slammming forces is expected to be partially caused by the difference in the waves, as shown in the figures.

The difference in the waves is also reflected in the measured response forces. The 1st waves in each run led to very low dynamic response forces, which implies that the waves were not broken at the structure as expected. The 2nd and 20th waves led to very unstable results due to the transient status of the starting and the ending of the test runs. Although the wave periods of the 18th wave and the 19th wave are higher than those of the other waves, there is no obvious effect on the response forces.

As long as the wave response forces are valid, more data points lead to a more informative statistical analysis, so the response forces from the 3rd to 19th waves in each run were used for the slamming force reconstruction. The data from each of the 46 hammer

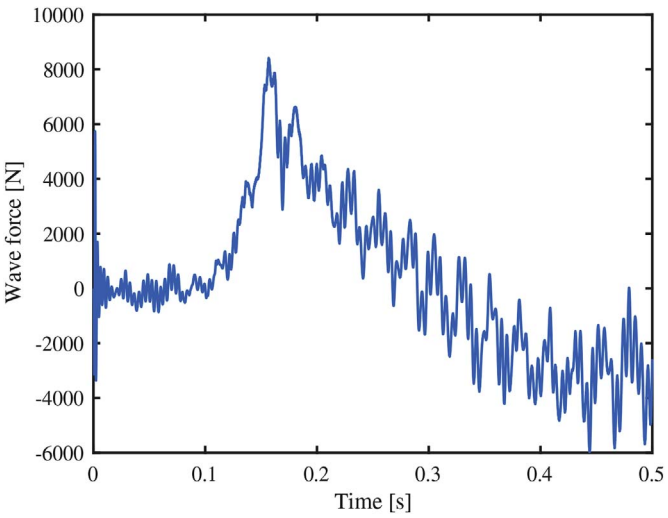

Fig. 8. Estimated wave slamming force.

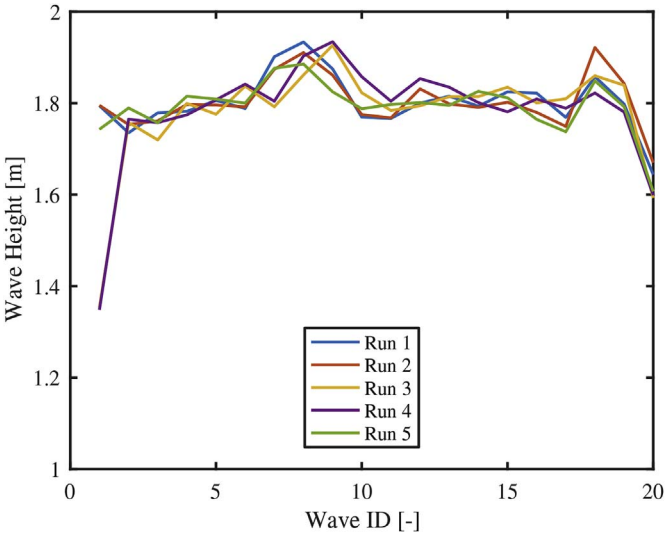

Fig. 9. Wave height variation over different runs and waves.

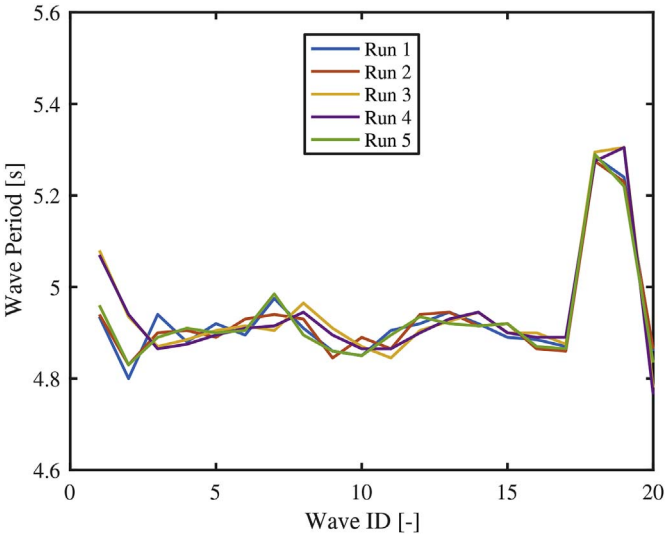

Fig. 10. Wave period variation over different runs and waves.

hits (see Table 3) were combined with the response force from each used wave for reconstructing the slamming force independently – the resulting forces are then averaged, as explained in Section 4.1.2. All together 46 (hits) × 5 (runs) × 17 (waves) = 3910 time series of the slamming forces were reconstructed. Statistical analysis is conducted for these slamming forces in this section, to better understand the variability of the estimated forces.

4.1. Analysis methods

Two basic methods used for the analysis are introduced, namely parametrization and multi-level analysis. Parametrization enables a statistical analysis of the slamming forces by using representative parameters that describe the main features of the force time series. Multi-level analysis is then used to average the results at various steps in the analysis, depending on which source of variability is investigated.

4.1.1. Parametrization

Since a large number of time series cannot be compared and analyzed directly, six parameters are assigned to each time series to describe the slamming forces, as illustrated in Fig. 11.

- F_p: Peak force, the maximum force in the time series.

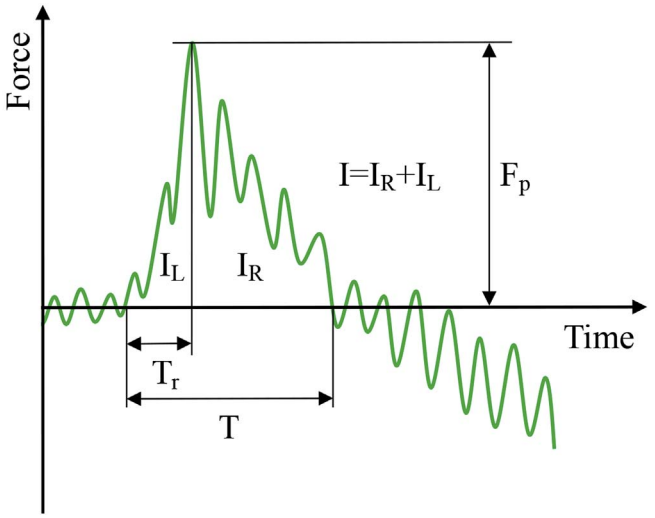

Fig. 11. Parameters to describe one wave slamming force time series. The variation of the time series has been exaggerated for visualization purposes.

- T: Duration, the time between the last zero-up-crossing before the peak and the first zero-down-crossing after the peak.
- T_r: Rising time, the time between the last zero-up-crossing before the peak and the peak itself.
- I: Impulse, the integral of the force over the duration.
- I_L: Left impulse, the integral of the force over the rising time.
- I_R: Right impulse, the integral of the force over the time between the peak and the first zero-down-crossing after the peak.

4.1.2. Multi-level analysis

The reconstructed slamming forces are organized according to the data hierarchy, as shown in Fig. 12. The total result is composed of the result calculated from 5 × 17 wave response forces. The result from each wave response force is composed of the results from hammer test data at 12 locations. The result from each hammer test location is composed of the results from different hits.

For the analysis in Section 4.2, averaging at three levels is introduced. The symbol X represents an arbitrary parameter describing the slamming force. The subscripts h, l, w, r, represent the indices of hit, location, wave and run, respectively.

- Average 1: Averaging the result from different hits for one location.

$$X_{r,w,l} = \frac{1}{N_h(l)} \sum_{h=1}^{N_h(l)} X_{r,w,l,h} \tag{12}$$

The number of hits $N_h(l)$ depends on the location (see Table 3).

- Average 2: Averaging the result from different locations for one wave.

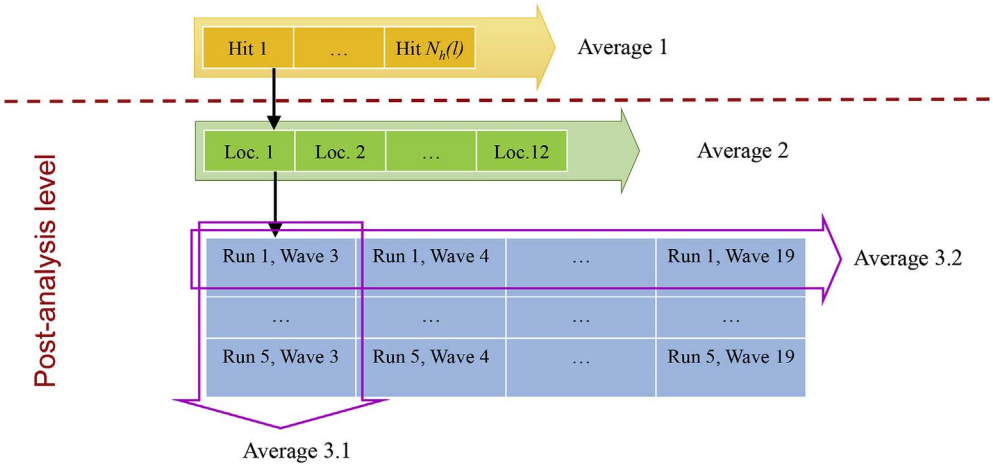

Fig. 12. Illustration of multi-level analysis.

$$X_{r,w} = \frac{1}{12}\sum_{l=1}^{12} X_{r,w,l} \tag{13}$$

- Average 3.1: Averaging the result from the same waves but over different runs.

$$X_w = \frac{1}{5}\sum_{r=1}^{5} X_{r,w} \tag{14}$$

- Average 3.2: Averaging the result from the same runs but for different waves.

$$X_r = \frac{1}{17}\sum_{w=3}^{19} X_{r,w} \tag{15}$$

Since the number of hammer hits is different depending on the location, a post-analysis level (see Fig. 12) is further defined to eliminate the difference due to unequal weights. The time series of the reconstructed force are averaged over different hits at each location. The peaks of the time series are aligned for the averaging. In the post-analysis level, these averaged time series are used, so that the forces at different locations carry the same statistical weight. A total of $12 \times 17 \times 5 = 1020$ averaged time series are available for analysis in this level. The discussions in Section 4.3 onward are all based on the results in the post-analysis level.

4.2. Variation features

Ideally, the slamming forces under the same wave condition should be identical. However, each wave in the experiment is different even under the same preset condition. Also, each group of hammer test data used for the force reconstruction is different, from hit to hit, and from location to location. Therefore, the variation features of the reconstructed slamming forces at different levels need to be checked.

The variation at the hit level is represented by the mean calculated using Average 1 (see Section 4.1.2) and the corresponding standard error of the mean. The values are calculated for the six representative parameters (see Section 4.1.1), and for all locations and all waves. In Fig. 13, an exemplary result, which shows the hit variation for twelve locations using the 16th wave of the 4th run, is demonstrated by the blue error bars. The hit variation shows no signs of systematic biases (such as dependence on hammer hit location or significant asymmetry), and the results from Average 1 are considered to be appropriate estimates of the slamming forces at this level. In addition, no special pattern among the locations is observed if all the waves are checked.

The variation at the location level is represented by the mean calculated using Average 2 and the corresponding standard error of the mean. The location variation for the same wave is demonstrated by the red and orange lines in Fig. 13.

The variation at the wave level is represented by the mean calculated using Average 3.1 and the corresponding standard error of the mean. As shown in Fig. 14, the peak force, impulse and right impulse increase as the wave ID increases, i.e. for the later waves in each run. In contrary, the duration and rising time decrease slightly. The left impulse is almost constant. The difference among the waves may be caused by the accumulated diffraction and refraction in each run, which is observed in the video record of the experiment. As these effects, including also a potentially shifting breaking point, cannot be quantified easily, we consider these unknown effects as part of the uncertainties reported.

The variation at the run level is represented by the mean calculated using Average 3.2 and the corresponding standard error of the mean. As shown in Fig. 15, the result only varies slight among different runs, which means the test runs have a good repeatability.

4.3. Correlation features

The correlation matrix of the six parameters is calculated and shown in Table 4. For the purposes here, we assume correlations above 0.8 to be strong, and correlations between 0.4 and 0.8 to be moderate. According to the correlation matrix, the peak force F_p has negative linear relationships with the duration T and with the rising time T_r. This is in accordance with the trend observed for example in Fig. 14. The impulse I has moderate positive linear relationships both with F_p and with T. The rising time T_r has a stronger linear relationship with the left impulse I_L than with I. The left impulse I_L and the right impulse I_R have very low correlation, which suggests that these two parts of the impulse are independent and can be treated separately. In summary, these results indicate that the chosen parameters are not independent, which could lead to identification issues. However, the only strong correlation is between I and I_R. Therefore, they will not be used together in the proposed force models (see Section 6).

4.4. Distribution features

To illustrate the data distribution features of the six parameters, histograms are plotted in Fig. 16. The number of bins is set as 30 for all histograms. The data are further fit by various distributions. The names and parameters of the distributions that seem to result in the best match, as well as the log-likelihood of the fitting are shown in Table 5. The means and 95% bootstrap confidence intervals

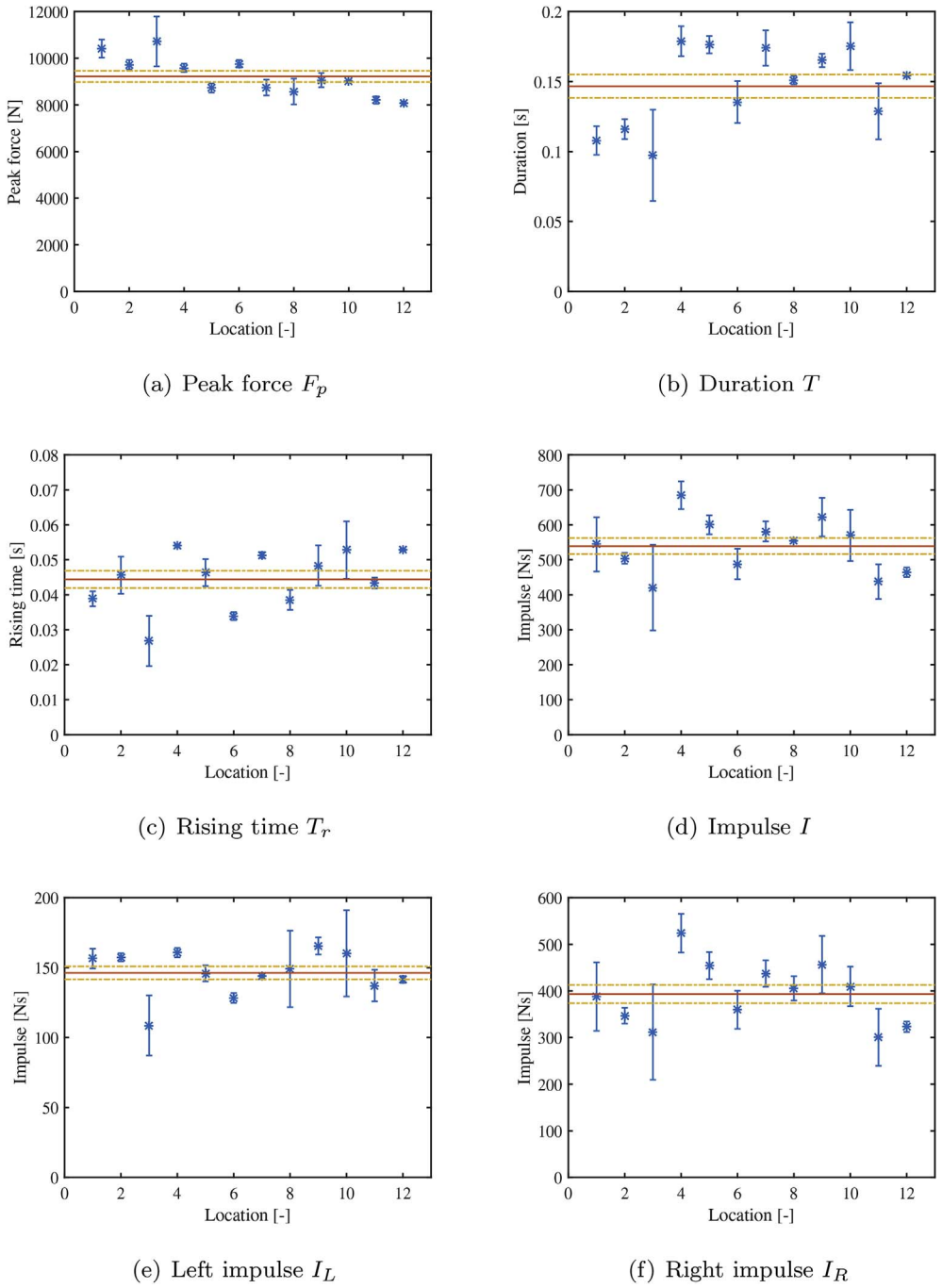

Fig. 13. Hit variation of the six parameters representing the slamming force (blue error bars indicate the standard error of the mean), and location variation of the six parameters representing the slamming force (red line indicates the mean, and orange lines indicate the standard error of the mean). The result shown is for the 16th wave of the 4th run, as a typical example. (For interpretation of the references to colour in this figure legend, the reader is referred to the web version of this article.)

[20] of the means based on 2000 bootstrap samples are marked in Fig. 16 and listed in Table 5.

4.5. Representative wave slamming force time series

Although the statistical properties of the representative parameters have been discussed thoroughly in the previous sections, a representative time series of the slamming force is still necessary to describe the force development in time. Therefore, a mean force time series is calculated according to Eq. (16) and shown in Fig. 17. The standard deviation of the data points at each time instance is

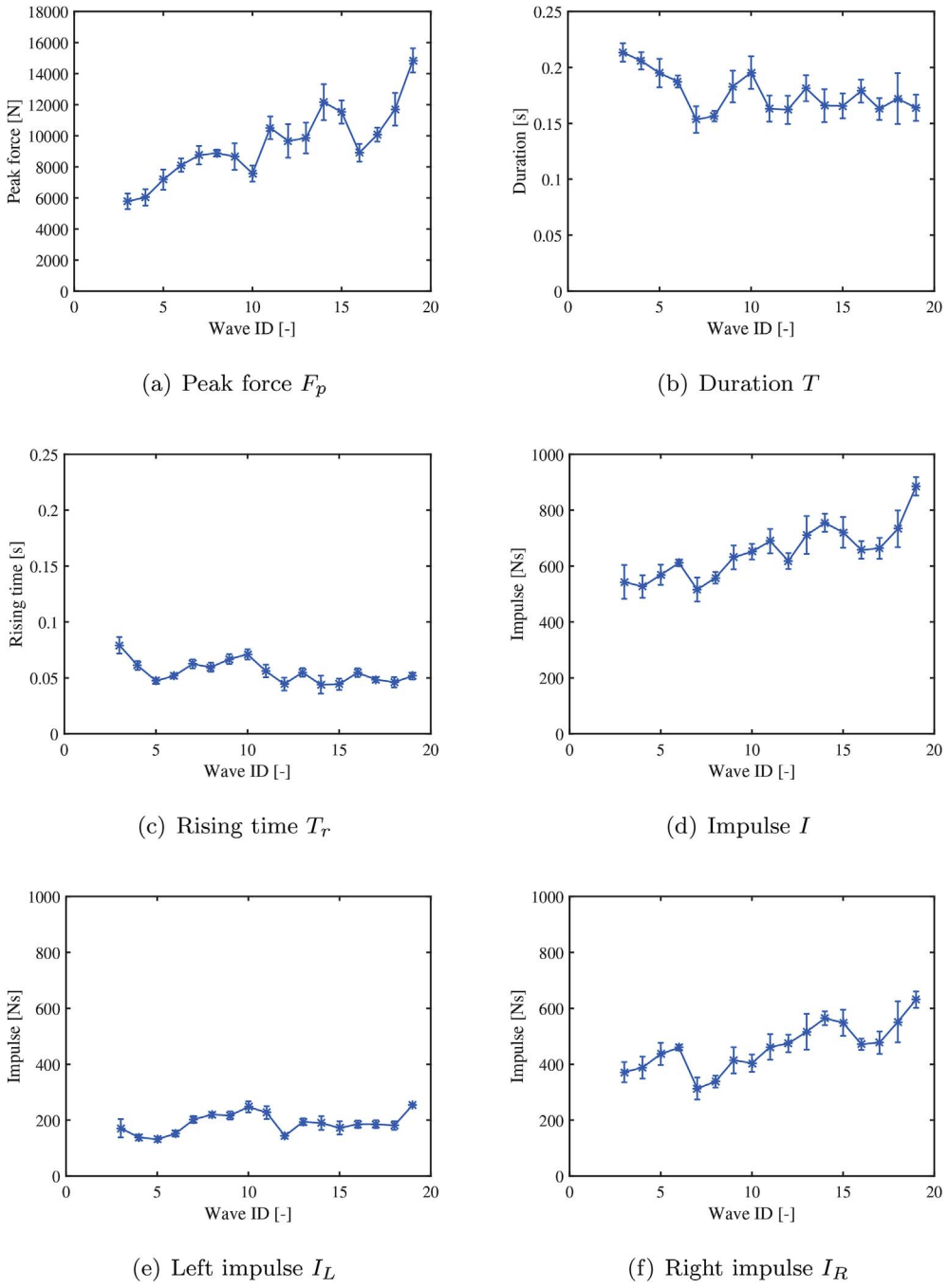

Fig. 14. Wave variation of the six parameters representing the slamming force.

also shown in the figure.

$$f_{rep}(t) = \frac{1}{12 \times 17 \times 5} \sum_{r=1}^{5} \sum_{w=3}^{19} \sum_{l=1}^{12} f_{r,w,l}(t) \tag{16}$$

5. Estimation of slamming coefficient

The slamming coefficient is an important factor to connect wave kinematics and slamming forces in engineering practice. It is essential for the calculation of the maximum slamming forces on a structure, given a certain wave condition. According to Goda et al.

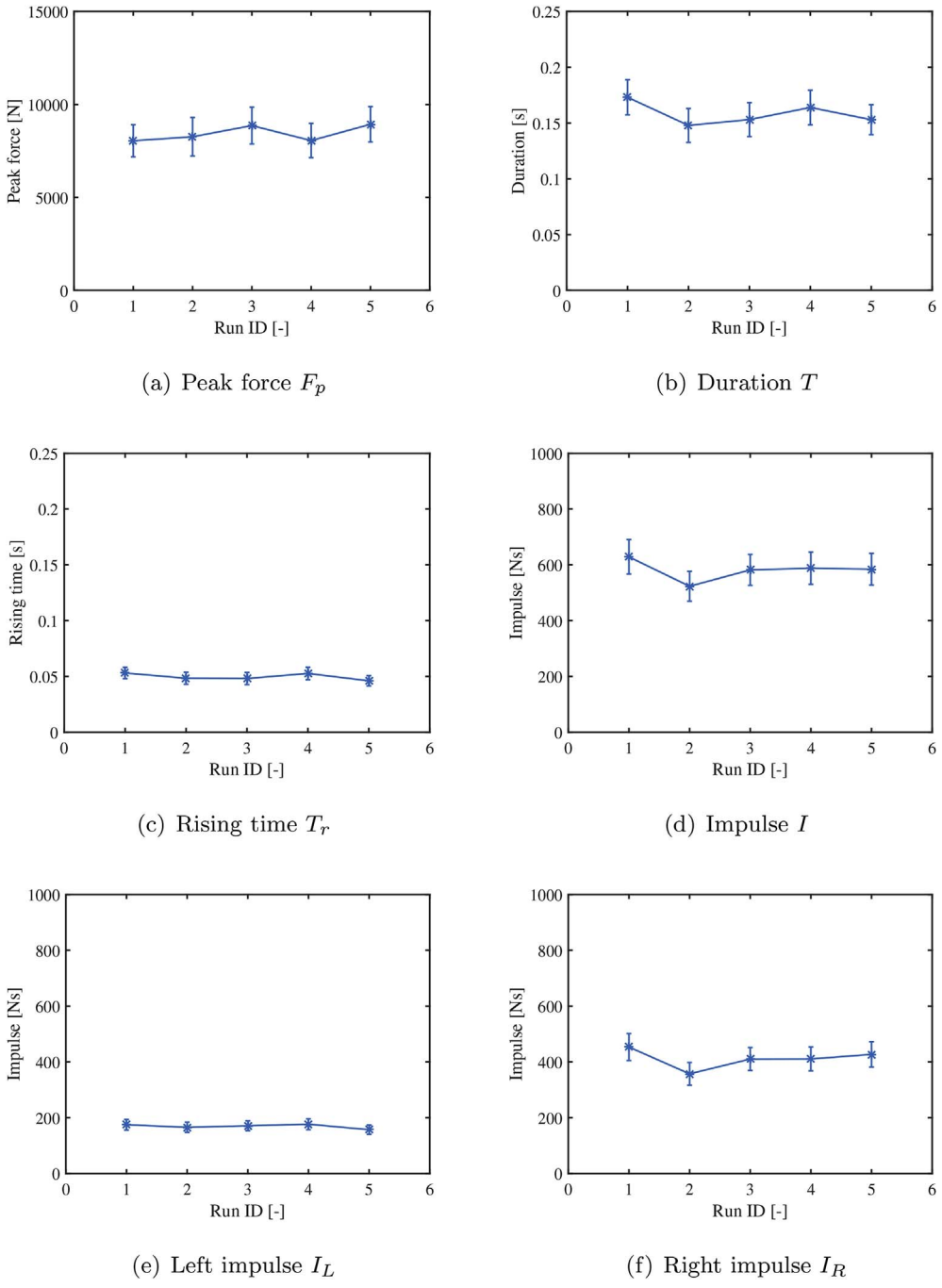

Fig. 15. Run variation of the six parameters representing the slamming force.

[21], the maximum wave slamming force on a cylinder is written as

$$F_s = \frac{1}{2}\rho_w C_s \lambda D \eta_b C_b^2 \tag{17}$$

where ρ_w is the water density, C_s the slamming coefficient, λ the curling factor, D the diameter of the cylinder, η_b the wave elevation and C_b the breaking wave celerity. When applying Eq. (17) on a jacket structure, D is interpreted as the width of the part that is exposed to the breaking wave. For the jacket structure considered in the WaveSlam project, D is estimated according to the geometry of the structure, as an expression of the diameter of the braces and the legs, $D = 2 \times (1 + 2.15) \times 0.14$ m$= 0.88$m. Each inclined brace contributes 2.15×0.14m to D, due to an inclined angle of 62° with respect to the vertical. The peak forces of the slamming force time series in the post-analysis level (see Section 4.1.2) are used as F_s for estimating the coefficient. The wave elevation η_b is taken as the

Table 4
Correlation matrix of the six parameters representing the slamming force.

	F_p	T	T_r	I	I_L	I_R
F_p	1.00	-0.42	-0.42	0.40	0.18	0.36
T	-0.42	1.00	0.53	0.53	0.10	0.55
T_r	-0.42	0.53	1.00	0.23	0.64	-0.07
I	0.40	0.53	0.23	1.00	0.46	0.89
I_L	0.18	0.10	0.64	0.46	1.00	0.01
I_R	0.36	0.55	-0.07	0.89	0.01	1.00

highest measured elevation of the corresponding wave. The breaking wave celerity is approximated by Ref. [22,23].

$$C_b = \sqrt{g(d + \eta_b)} \tag{18}$$

where g is the gravitational acceleration and d is the water depth. The curling factor λ is highly dependent on the wave properties and the type of structure, and it cannot be identified independently of C_s without further assumptions. Therefore, the slamming coefficient C_s is first estimated together with the curling factor, by using Eq. (17) with the estimated slamming forces.

For all used F_s, the product $C_s\lambda$ is estimated and its distribution is plotted in Fig. 18. The distribution is fit by a Gumbel distribution. The mean value of $C_s\lambda$ is about 0.515, and the corresponding 95% bootstrap confidence interval of the mean is [0.506, 0.525], as indicated in Fig. 18. Taking the mean value of $C_s\lambda$ and a range plus or minus one standard deviation, the variation of slamming coefficient is plotted against the curling factor ranging from 0.1 to 0.5 in Fig. 19. At the maximum curling factor proposed by Goda et al. [21] for plunging breaking waves, $\lambda = 0.4$, the mean slamming coefficient is approximately $C_s = 1.29$. Taking one standard deviation around the mean into account due to the data uncertainties, the slamming coefficient C_s ranges from around 0.70 to 6.78 for the range of curling factor from 0.1 to 0.5.

It should be noted that in the above estimation of slamming coefficient, the assumption on the width D may cause some uncertainty in the estimation of slamming coefficient C_s. Depending on the wave impact location, the actual effective diameter D may be slightly smaller than the used one due to the local geometry at the joints. The geometry of the jacket is very different from that of a cylinder, so the effective impact area is also somewhat different.

6. Wave slamming force models

When performing a dynamic analysis of a structure subjected to slamming forces, the time history of the slamming forces is usually required as an input. Proper wave slamming force models, which can simulate the time history of wave slamming force, are thus desirable. Two models are proposed in this section, based on the representative time series of wave slamming force shown in Fig. 17 and the values of the six parameters.

6.1. Simplified model

A three-parameter triangular force model, denoted as simplified model, is proposed, considering the correlation among the studied parameters (see Section 4.3):

$$f(t) = \begin{cases} F_p \frac{(t-(t_p-T_r))}{T_r} & t_p - T_r < t \le t_p \\ F_p \frac{(t_p - T_r + T - t)}{T - T_r} & t_p < t \le t_p - T_r + T \\ 0 & \text{Otherwise} \end{cases} \tag{19}$$

where t_p denotes the instant of peak force; F_p, T_r and T are the peak force, rising time and duration of the slamming force, respectively. By applying the mean values of these parameters estimated in Section 4.4, the simplified model is obtained, as plotted in Fig. 20 by a red line. For a more conservative estimation, the mean plus one standard deviation values of the parameters are used in the model. The result is shown in the same figure by a yellow line.

To verify the simplified model, the left impulse, I_L, and the right impulse, I_R, are calculated for the representative time series and the simplified model. Here the I_L and I_R are calculated over the range of $[t_p - Tr, t_p]$ and $[t_p, t_p - T_r + T]$, respectively. The results are given in Table 6. It can be found that the simplified model greatly overestimates the I_L and I_R by approximately 50.02% and 36.61%, respectively. Hence, a more refined model is desirable to describe the time series of wave slamming force.

6.2. Refined model

As observed in Fig. 17, the wave slamming force seemingly ascends exponentially until it reaches the peak; after that, it descends also exponentially. Therefore, two exponential curves are used to model the data at both sides of the peak more precisely. This refined model is thus proposed as follows:

$$f(t) = \begin{cases} F_p \exp\left(\alpha_1 \frac{t-t_p}{T_r}\right) & t_p - T_r < t \le t_p \\ F_p \exp\left(\alpha_2 \frac{t-t_p}{T-T_r}\right) & t_p < t \le t_p - T_r + T \\ 0 & \text{Otherwise} \end{cases} \tag{20}$$

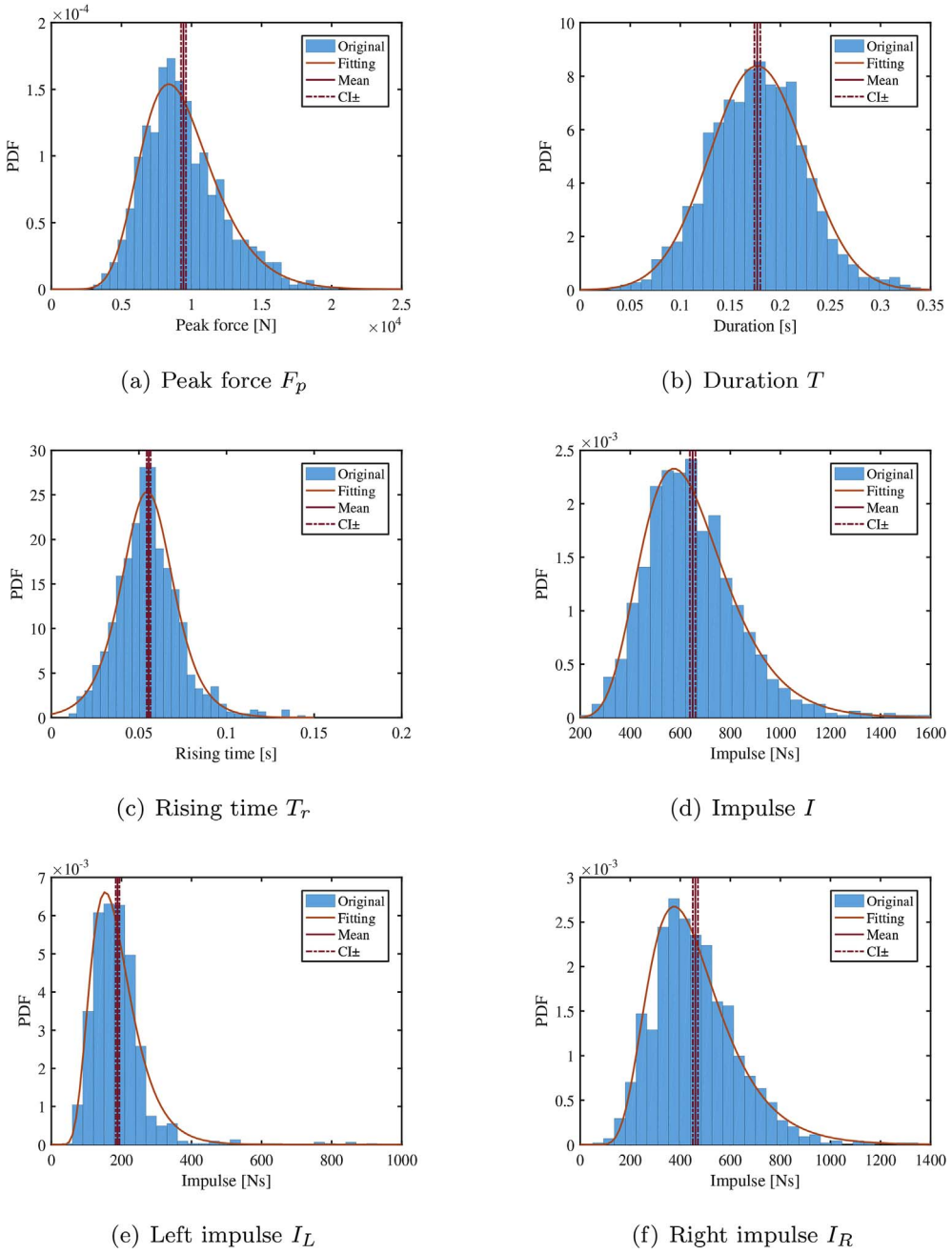

Fig. 16. Statistical properties of the six parameters representing the slamming force. Histogram, distribution, mean and confidence interval of mean are shown.

In addition to the three parameters, F_p, T_r and T, used in the simplified model, two coefficients α_1 and α_2 are introduced to indicate the rate of exponential decay on both sides of the peak. By using the mean values of the three parameters estimated in Section 4.4, the refined model is fit to the representative time series by employing a nonlinear least square curve fitting method. The results are demonstrated in Fig. 21 by a red line, and the fit coefficients are $\alpha_1 = 2.79$ and $\alpha_2 = -2.36$. The curve on the left side of the peak has a higher rate of decay than the curve on the right side, which is reflected by a higher absolute value of α_1 than α_2. For a more conservative estimation, the mean plus one standard deviation values of the three parameters are used, while α_1 and α_2 are kept the same. The result is shown in the same figure by a yellow line.

Similarly, the left impulse, I_L, and the right impulse, I_R, are estimated to verify this refined model, as given in Table 6. The relative errors of I_L and I_R between the representative time series and the refined model are 0.89% and 4.50%, respectively, which implies that this refined model represents the wave slamming force time series fairly well.

The refined model has a more accurate match with the representative time series, while the simplified model leads to a more

Table 5
Mean, confidence interval of mean and distribution of the six parameters representing the slamming force.

	F_p [N]	T [s]	T_r [s]	I [Ns]	I_L [Ns]	I_R [Ns]
Mean	9425.2	0.177	0.056	649.4	189.0	460.3
Confidence interval of the mean (lower limit)	9273.9	0.174	0.054	638.5	184.1	449.8
Confidence interval of the mean (upper limit)	9618.3	0.180	0.057	661.6	194.9	470.7
Fit distribution	Gumbel	Normal	Logistic	Log-normal	Log-normal	Log-normal
Distribution parameters*	$\sigma = 2395.7$ $\mu = 8196.9$ $k = -0.072$	$\sigma = 0.048$ $\mu = 0.177$	$\sigma = 0.010$ $\mu = 0.055$	$\sigma_L = 0.29$ $\mu_L = 6.44$	$\sigma_L = 0.37$ $\mu_L = 5.17$	$\sigma_L = 0.37$ $\mu_L = 6.07$
Log-likelihood of fitting	−9505.8	1659.5	2666.6	−6734.9	−5696.2	−6622.2

*σ = scale factor, μ = location factor, k = shape factor, σ_L = log scale factor, μ_L = log location factor.

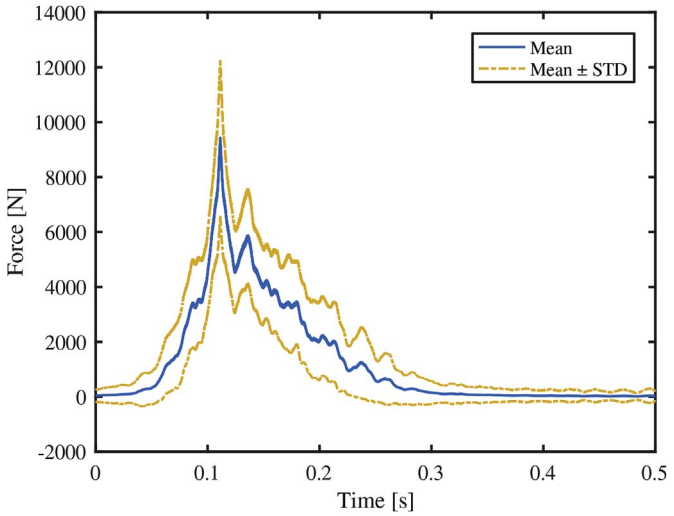

Fig. 17. Representative mean wave slamming force time series and its standard deviation.

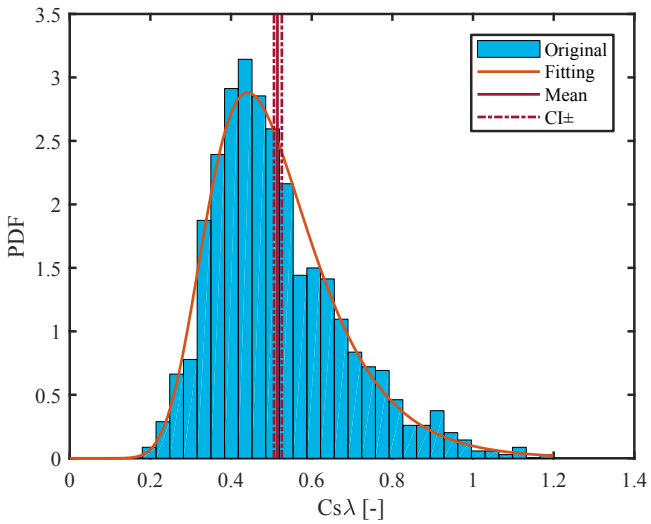

Fig. 18. Statistical properties of $C_s\lambda$, represented by histogram, Gumbel distribution fit, mean and confidence interval of the mean.

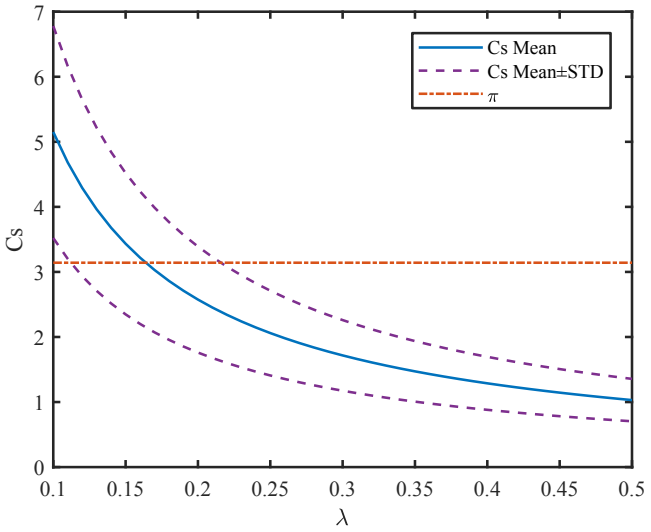

Fig. 19. C_s under different λ values.

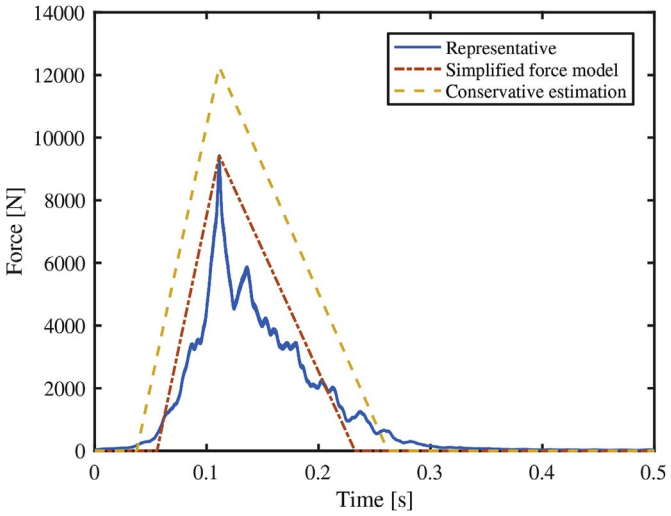

Fig. 20. Simplified force model for the representative wave slamming force time series.

conservative estimation of the impulse. On the other hand, the simplified model only requires three parameters. It is easier to be applied in practice, compared to the refined model, which requires two more parameters that are sensitive to the data.

7. Conclusions and outlook

This study aimed at investigating the global slamming forces due to plunging breaking waves on jacket structures, based on the statistical analysis of the experimental data from the WaveSlam project.

A total of 3910 time series of slamming forces were reconstructed based on the hammer test data and wave test data. To reveal the characteristics of the slamming force, six parameters were introduced to describe each force time series, including the peak force, duration, impulse, rising time, left impulse, and right impulse. The variation, correlation and distribution features of these parameters were investigated. High variability of these parameters is observed. Strong correlation is only found between the impulse and right impulse. A representative wave slamming time series was obtained by averaging all the reconstructed time series with respect to location, wave and run.

The statistical analysis serves as a basis for the estimation of slamming coefficient and the setup of force models. Taking one standard deviation around the mean into account due to the data uncertainties, the slamming coefficient C_s ranges from around 0.70 to 6.78 for the range of curling factor from 0.1 to 0.5. If the curling factor is set to 0.4, the mean C_s is approximately 1.29. Based on the representative slamming force time series, a 3-parameter triangular force model and a 5-parameter exponential force model were proposed to represent the time series of wave slamming force.

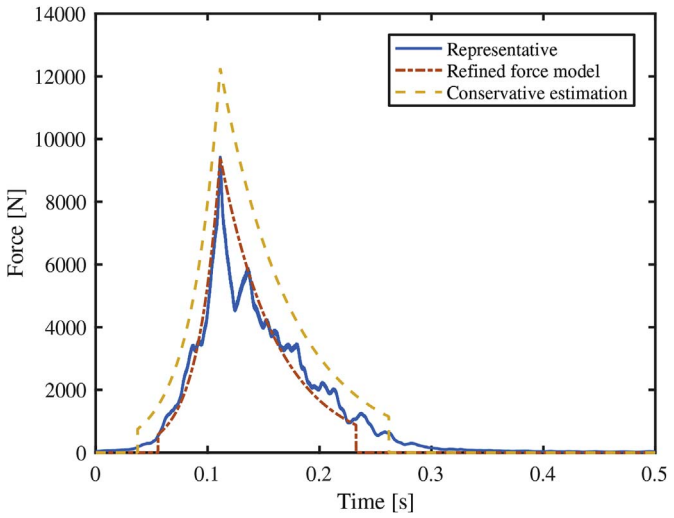

Fig. 21. Refined force model for the representative wave slamming force time series.

Table 6
The estimated impulse I_L and I_R by using the representative time series, simplified model and refined model.

	Rep. time series	Simplified model		Refined model	
	Value [Ns]	Value [Ns]	Error [%]	Value [Ns]	Error [%]
I_L	174.48	261.76	50.02	176.04	0.89
I_R	417.68	570.63	36.61	436.48	4.50

It should be noted that this paper statistically studied the global slamming forces on a jacket structure under one exemplary wave condition, more wave conditions should be investigated in the future to verify the slamming coefficient and the proposed wave models. The results in this study can also be verified by using an finite element model of the jacket structure, with careful consideration of the modeling strategies for various measurement devices and joints. For cylindrical structures, the slamming coefficient estimated from the Von Karman or Wagner theory is π or 2π and is not related to the curling factor. For the jacket structure considered in this paper, the slamming coefficient is dependent on the curling factor, because only the product $C_s\lambda$ is identified. The resulting slamming coefficient is therefore given as a range and different from that of cylindrical structures. Given a commonly used curling factor, $\lambda = 0.4$, the resulting C_s is significantly lower than the corresponding values for cylinders, because the breaking waves do not hit different parts of the jacket simultaneously. This result is important for the design of the structures, since it leads potentially to more economical jackets. Although only one jacket structure is considered in this paper, it is a typical jacket structure for offshore wind applications. The results are therefore valuable for slamming load considerations in the design of similar jacket structures.

For safe design of structures, the uncertainties of the external loads should be taken into account properly. The uncertainties of slamming loads not only result from the long term and short term wave statistics, but also arise from statistical variations under each wave condition. This study reveals the uncertainties of the slamming loads under one controlled wave condition in the laboratory. So far, this contribution to the uncertainties has mostly been neglected in the literature. Yet, as the present work shows, these variations are important. Using the slamming load distribution under one wave condition, together with the long term and short term distributions of wave conditions, it will be possible to determine a probability distribution of slamming loads. This could then be used to evaluate structural reliability and thereby serve as basis for probabilistic design of structures.

The challenges, of course, are the determination of the statistics of breaking wave conditions and slamming loads that occur in irregular wave conditions. The substructure geometry and bathymetry may also be different. Addressing the statistics of the slamming loads in such generality is very challenging, especially given the limitations of experimental data, where only a few of all possible parameters can be varied. Of course, the change from a single cylinder to a multi-element jacket structure – the topic of our study – results in effects that are also relevant for other multi-element structures. We therefore expect that the proposed model could also, with slight modifications, be used with other multi-element structures. Without further knowledge of the slamming loads under different wave conditions, one might use Eq. (17) with the identified $C_s\lambda$ values to obtain a first estimate of these loads. However, the suitability and accuracy of this approach still needs to be investigated. The biggest uncertainty when designing for breaking waves, however, still seems to be determining the long-term distribution of irregular breaking waves, i.e. which breaking waves are expected under a given irregular sea state, for a certain site and bathymetry. We hope that these issues will be addressed in the future.

Acknowledgment

This work has been supported by the European Community's Seventh Framework Programme through the grant to the budget of the Integrating Activity HYDRALAB IV within the Transnational Access Activities, Contract no. 261520.

Additional financial support from NOWITECH FME (Research Council of Norway, contract no. 193823) is gratefully acknowledged.

References

[1] Hallowell S, Myers AT, Arwade SR. Variability of breaking wave characteristics and impact loads on offshore wind turbines supported by monopiles. Wind Energy 2016;19(2):301–12. http://dx.doi.org/10.1002/we.2000.
[2] International Electrotechnical Commission (IEC). IEC 61400–61403, Wind turbines - part 3: design requirements for offshore wind turbines. 1.0 ed. 2009.
[3] Det Norske Veritas (DNV). DNV-OS-J101, Offshore standard: design of offshore wind turbine structures. 2014.
[4] GL Renewables Certification. Guideline for the certification of offshore wind turbines. 2012.
[5] Faltinsen O. Sea loads on ships and offshore structures. Cambridge University Press; 1993.
[6] Alagan Chella M, Tørum A, Myrhaug D. An overview of wave impact forces on offshore wind turbine substructures. Energy Procedia 2012;20:217–26. http://dx.doi.org/10.1016/j.egypro.2012.03.022.
[7] Ridley JA. A study of some theoretical aspects of slamming. Technical Report. National Maritime Institute, UK: NMI R158; 1982.
[8] Perlin M, Choi W, Tian Z. Breaking waves in deep and intermediate waters. Annu Rev Fluid Mech 2013;45:115–45. http://dx.doi.org/10.1146/annurev-fluid-011212-140721.
[9] Wienke J, Oumeraci H. Breaking wave impact force on a vertical and inclined slender pile - theoretical and large-scale model investigation. Coast Eng 2005;52:435–62. http://dx.doi.org/10.1016/j.coastaleng.2004.12.008.
[10] Irschik K, Sparboom U, Oumeraci H. Breaking wave loads on a slender pile in shallow water. Proceedings of 29th international conference on coastal engineering. Lisbon, Portugal. 2004.
[11] Bredmose H, Slabiak P, Sahlberg-Nielsen L, Schlütter F. Dynamic excitation of monopiles by steep and breaking waves: experimental and numerical study. Proceedings of 32nd International Conference on Ocean, Offshore and Arctic Engineering. Nantes, France. 2013.
[12] Rausa IE, Muskulus M, Arntsen ØA, Wåsjø K. Characterization of wave slamming forces for a truss structure within the framework of the WaveSlam project. Energy Procedia 2015;80:276–83. http://dx.doi.org/10.1016/j.egypro.2015.11.431.
[13] Tu Y, Muskulus M, Arntsen ØA. Experimental analysis of slamming load characteristics for truss structures in offshore wind applications. J Ocean Wind Energy 2015;2(3):138–45. http://dx.doi.org/10.17736/jowe.2015.jcr32.
[14] Jose J, Podrazka O, Obhrai C, Gudmestad OT, Cieslikiewicz W. Methods for analysing wave slamming loads on truss structures used in offshore wind applications based on experimental data. Int J Offshore Polar Eng 2016;26(2):100–8. http://dx.doi.org/10.17736/ijope.2016.mkr05.
[15] Tu Y, Muskulus M, Grindstad TC. Two methods for the inverse estimation of local slamming loads on a jacket structure. Proceedings of 35th International Conference on Ocean, Offshore and Arctic Engineering. Busan, South Korea. 2016.
[16] Arntsen Ø, Obhrai C, Gudmestad O. Data storage report: wave slamming forces on truss structures in shallow water. Technical Report, WaveSlam (HylV-FZK-05). Norwegian University of Science and Technology; 2013.
[17] Tørum A. Wave slamming forces on truss structures in shallow water. Technical Report Norwegian University of Science and Technology; 2011. Version 2011-10–03.
[18] Aune L. Forces from plunging breaking waves on a truss structure Master thesis Norwegian University of Science and Technology; 2011
[19] Cleveland WS. Robust locally weighted regression and smoothing scatterplots. J Am Stat Assoc 1979;74(368):829–36. http://dx.doi.org/10.1080/01621459.1979.10481038.
[20] Efron B. Bootstrap methods: another look at the jackknife. Ann Statistics 1979;7(1):1–26. http://dx.doi.org/10.1214/aos/1176344552.
[21] Goda Y, Haranaka S, Kitahata M. Study of impulsive breaking wave forces on piles. Rep Port Harbour Tech Res Inst 1966;6(5):1–30.
[22] Tanimoto K, Takahashi S, Kaneko T, Shiota K. Impulsive breaking wave forces on an inclined pile exerted by random waves. Coast Eng Proc 1986;1(20):2288–302. http://dx.doi.org/10.1061/9780872626003.168.
[23] Mei CC, Stiassnie M, Yue DK. Theory and applications of ocean surface waves: nonlinear aspects. World Scientific; 2005.